

Enabling Instructional Image Editing with In-Context Generation in Large Scale Diffusion Transformer

Zechuan Zhang, Ji Xie, Yu Lu, Zongxin Yang, Yi Yang[†]

ReLER, CCAI, Zhejiang University

Project Page: <https://river-zhang.github.io/ICEdit-gh-pages>

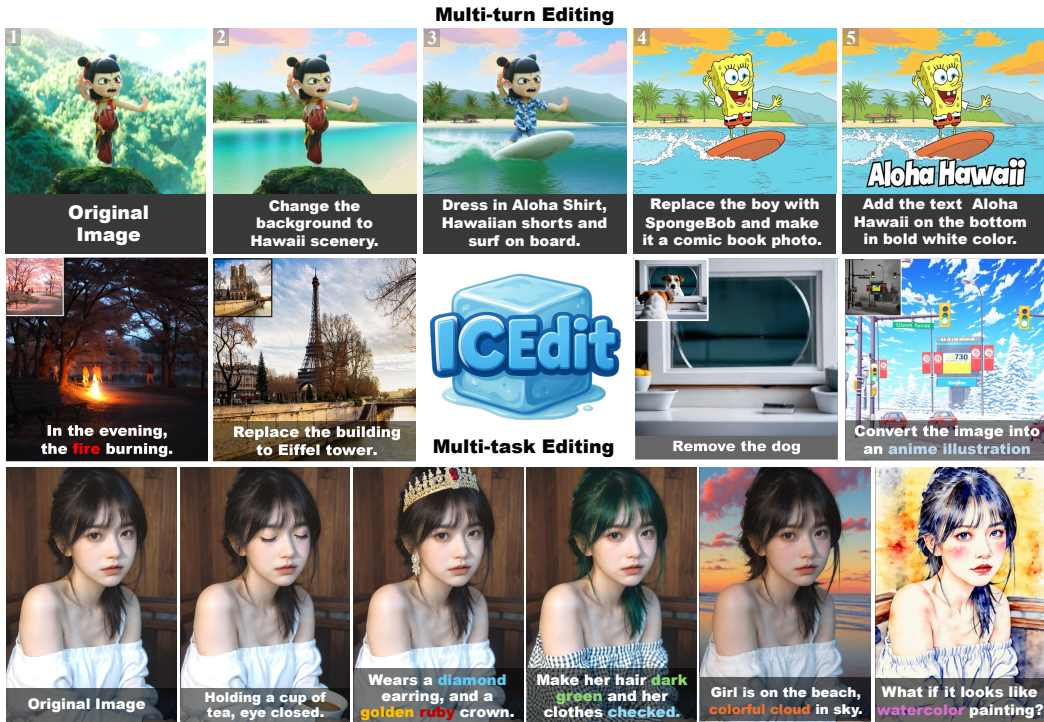


Figure 1: We introduce ICEdit, a novel method that achieves state-of-the-art instruction-based image editing with only 0.1% training data required by previous SOTA methods, demonstrating exceptional generalization. The first row illustrates a series of multi-turn edits, executed with high precision, while the second and third rows highlight diverse, visually impressive editing results from our method.

Abstract

Instruction-based image editing enables precise modifications via natural language prompts, but existing methods face a precision-efficiency tradeoff: fine-tuning demands massive datasets ($>10M$) and computational resources, while training-free approaches suffer from weak instruction comprehension. We address this by proposing **ICEdit**, which leverages the inherent comprehension and generation abilities of large-scale Diffusion Transformers (DiTs) through three key innovations: (1) An in-context editing paradigm without architectural modifications; (2) Minimal parameter-efficient fine-tuning for quality improvement; (3) Early Filter Inference-Time Scaling, which uses VLMs to select high-quality noise samples for efficiency.

Experiments show that ICEdit achieves state-of-the-art editing performance with only 0.1% of the training data and 1% trainable parameters compared to previous methods. Our approach establishes a new paradigm for balancing precision and efficiency in instructional image editing.

1 Introduction

In recent years, instruction-based image editing has gained considerable attention for its ability to transform and manipulate images using natural language prompts. The main advantage of instruction-based editing is its ability to generate precise modifications with minimal textual instructions, thereby opening new possibilities for both automated image processing and user-driven content creation.

Instruction-based image editing methods are divided into finetuning-based [1, 2, 3, 4, 5, 6, 7, 8, 9, 10] and training-free approaches [11, 12, 13, 14, 15, 16, 17, 18, 19]. Finetuning-based methods achieve precise instruction-following by fully finetuning pretrained diffusion models on large-scale datasets (450K to 10M samples [1, 3]) with structural modifications like condition embedding [9, 5] or channel adjustments [1, 2, 4], but demand significant computational resources. In contrast, training-free methods avoid retraining through techniques like image inversion, or attention manipulation, offering efficiency but struggling with complex instructions, which reduces precision and practical utility. This highlights a **critical trade-off between precision and efficiency** in current methods.

Despite the dilemma above, recent advances in diffusion transformers (DiT) [20, 21, 22] suggest a promising pathway. DiT architectures exhibit two critical properties: (1) **Scalable Generation Fidelity**: Larger DiT variants (e.g., FLUX [23]), trained on vast amounts of image-text data, possess unprecedented text-to-image alignment capabilities. (2) **Intrinsic Contextual Awareness**. Diffusion Transformers (DiTs) leverage attention mechanisms to enable bidirectional interactions between reference and generated content, processing source and target images concurrently. This facilitates tasks like reference-guided synthesis [24, 25] and identity-preserved editing [26], while supporting conditional image generation without specialized alignment networks [27, 7, 28].

Although these works achieve promising results, they are unsuitable for instruction-guided image editing due to their limited ability to comprehend explicit editing instructions and preserve the layout of non-editable regions. This raises a critical question: **Can large scale DiT’s generation capacity and contextual awareness directly address instruction-based image editing, while balancing precision and efficiency through intrinsic capabilities rather than external complexity?**

Our experiments reveal two fundamental limitations in using DiTs for instructional image editing: (1) **Poor instruction comprehension**: while the model can interpret descriptive input/target prompts, it struggles with direct editing instructions (e.g., "make it..." or "change it..."); (2) **Layout instability**: the model often alters unchanged regions when regenerating scenes, leading to poor editing success.

To address these limitations, we suggest a two-part solution. First, we recommend turning direct editing commands into descriptive prompts that match how DiTs naturally understand information. Second, the editing challenges mainly arise from the model’s unlearned image-to-image editing priors, which can potentially be addressed through lightweight fine-tuning with editing pairs or test-time adaptation [29, 30] strategies. This approach offers the potential to simultaneously resolve DiTs’ two fundamental limitations in instructional editing while maintaining precision-efficiency balance.

In this paper, we propose **ICEdit, an efficient and effective framework** for instructional image editing that directly exploits the inherent comprehension and generative capabilities of large-scale DiT priors for instructional image editing. Our approach employs in-context prompts—a fixed-format prefix embedding editing instructions in a format DiT can effectively interpret (§3.1). Given a source image (left panel), the model generates edited outputs (right panel) by jointly processing these prompts and the input (see fig. 2(a) and fig. 5). Moreover, minimal parameter-efficient fine-tuning significantly improves editing success and quality, while adopting a Mixture-of-Experts (MoE) [31] further enhances performance (§3.2). Finally, we introduce *Early Filter Inference-Time Scaling*, which uses vision-language models (VLMs) to evaluate noise quality during early denoising stages in rectified flow models (§3.3). This method rapidly identifies and filters out noises congruent with textual instructions, enhancing robustness and output fidelity.

We evaluate our method on the Emu Edit [3] and MagicBrush [2] benchmarks, demonstrating three key advancements: **Significant Data Efficiency and Editing Quality**: Achieving state-of-the-art

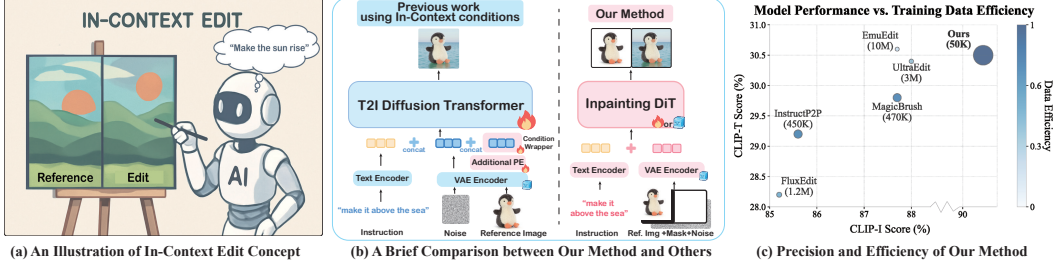


Figure 2: (a) Our concept: The original DiT model is conceptualized as a painter who generates edited images (right panel) by interpreting the reference image (left panel) and the instruction, similar to finishing an artwork based on a provided sketch. (b) Comparison of model structures: Unlike prior DiT methods, our approach avoids extra position/condition encoders, easily and effectively preserving the original model structure. (c) Our method leverages minimal training data and achieves comparable performance with SOTA models.

results with minimal training data (0.1% of prior requirements). **Validation of Proposed Paradigm:** Outperforming recent DiT-based editing models (both T2I and inpainting variants), confirming the effectiveness of our in-context editing approach. **Practical Applicability:** Attaining a competitive VIE score of **78.2** (compared to SeedEdit’s 75.7), demonstrating real-world viability comparable to commercial systems. These results establish a novel perspective on balancing precision and efficiency (fig. 2(c)) by leveraging large-scale DiTs as priors. Our contributions include:

- We explore the editing ability of large pretrained DiTs and propose an in-context editing paradigm, ICEdit, that enables instructive image editing by leveraging the model’s inherent understanding and generation abilities, without requiring architectural modifications or extensive fine-tuning.
- Our framework demonstrates significant improvements through minimal fine-tuning, significantly enhancing editing quality and robustness. We further propose an *Early Filter Inference-Time Scaling* approach that uses VLM to select high-quality noise samples. This integrated strategy improves editing precision while maintaining computational efficiency.
- Experimental results show that our method **achieves state-of-the-art editing performance while requiring only 0.1% of the training data compared to previous approaches**, establishing a novel perspective on balancing precision and efficiency.

2 Related Work

Training-free editing techniques. Since the emergence of Diffusion Models, numerous training-free image editing methods [11, 32, 19, 33, 15, 17, 16, 13] have gained attention. Recently, RF-Solver [13] improves inversion precision in Rectified-flow models by mitigating ODE-solving errors and leverages MasaCtrl [19] for image editing. StableFlow [14] identifies critical MM-DiT Blocks through ablation studies, injecting features only into these blocks to enhance editing capabilities. However, these methods face two key limitations: 1) manually designed modules restrict generation ability, hindering complex instruction understanding and reducing success rates; 2) editing requires carefully crafted prompts, limiting generalizability and scalability.

Finetuning-based editing methods. Most current editing models modify architectures and fine-tune on high-quality datasets [1, 2, 34, 4, 35, 10, 8]. InstructPix2Pix [1], MagicBrush [2], and UltraEdit [4] fine-tune diffusion UNet using original images as input. MGIE [5] and SmartEdit [9] enhance instruction understanding by integrating a Multimodal Large Language Model (MLLM) to encode and inject instructions into the diffusion model. However, **a gap exists between the embedding spaces of generative prompts and editing instructions**, reducing the generalization ability of Diffusion Models and necessitating large datasets to bridge it. For instance, InstructPix2Pix generated 450K pairs, Emu Edit [3] collected nearly 10M pairs, and FluxEdit [36] used 1.2M pairs from [34] based on FLUX [23], yet the editing results remain suboptimal.



Figure 3: **Input Prompt Variants for Image Editing.** We evaluate three prompt formats: (1) Direct Instruction - explicit editing commands provided directly; (2) In-context Prompt - instructions embedded in structure "A diptych with... On the right, the same scene but {instruction}"; (3) Global Descriptive Prompt - uses full input/output captions ("On the left {input} On the right {output}").

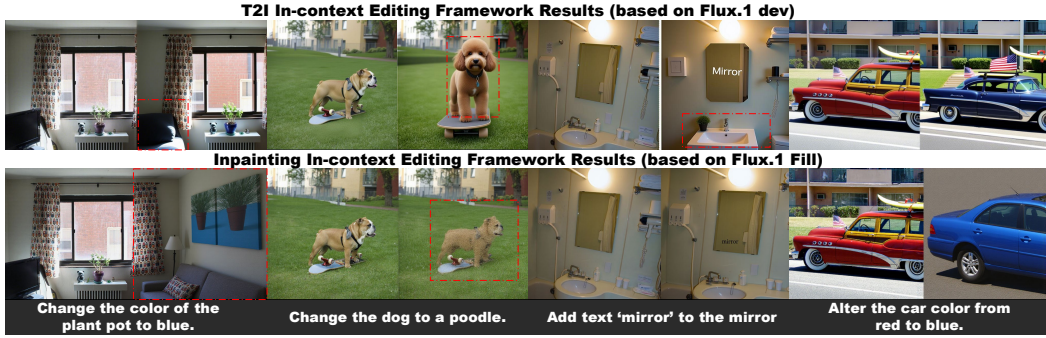


Figure 4: **Training-Free Methods Show Limited Performance.** Both T2I and inpainting DiT frameworks (fig. 5) yield suboptimal results. The T2I DiT struggles to preserve the original layout, while the inpainting framework may inadvertently perform outpainting. Despite these shortcomings, both demonstrate potential in following instructions and modifying edited regions.

3 Method

In this section, we first explore in-context editing capabilities within original DiT generative models and propose our **in-context edit framework** for instruction-based image editing (§3.1). After thorough analysis, we perform minimal fine-tuning to significantly improve editing quality and robustness of our editing paradigm (§3.2). Finally, we present **early filter inference-time scaling** (§3.3) to optimize initialization noise for better generation quality.

3.1 Exploration of DiT’s In-context Edit Ability

In-Context Edit Framework. Inspired by recent advances in large-scale Diffusion Transformer (DiT) models [27, 26, 37, 24], which demonstrate robust contextual capabilities, we investigate image editing via in-context generation. As illustrated in fig. 2(a), our approach mimics an AI painter that generates edited images (right panel) by interpreting a reference image (left panel) and an edit instruction. By leveraging DiT’s strong generation fidelity and inherent contextual awareness, we aim to enable direct image editing without requiring module modifications or extensive finetuning.

We propose two training-free frameworks based on text-to-image (T2I) DiT and inpainting DiT, respectively, as shown in fig. 5(a). For the T2I DiT framework, we introduce an implicit reference image injection method. We perform image inversion [38, 13, 14, 19, 18] on the reference image, preserving attention values across layers and steps. These values are injected into tokens representing the left side of a diptych for image reconstruction, while the right side is generated based on the edit instruction within a predefined prompt during in-context generation.

Conversely, the inpainting DiT framework offers a more straightforward approach. By accepting a reference image, we construct a side-by-side image, where the left-hand side is reconstructed as a reference image, and the right-hand side is the "edited" result. The whole process is guided by a **fixed mask** and an edit prompt to produce the edited output.

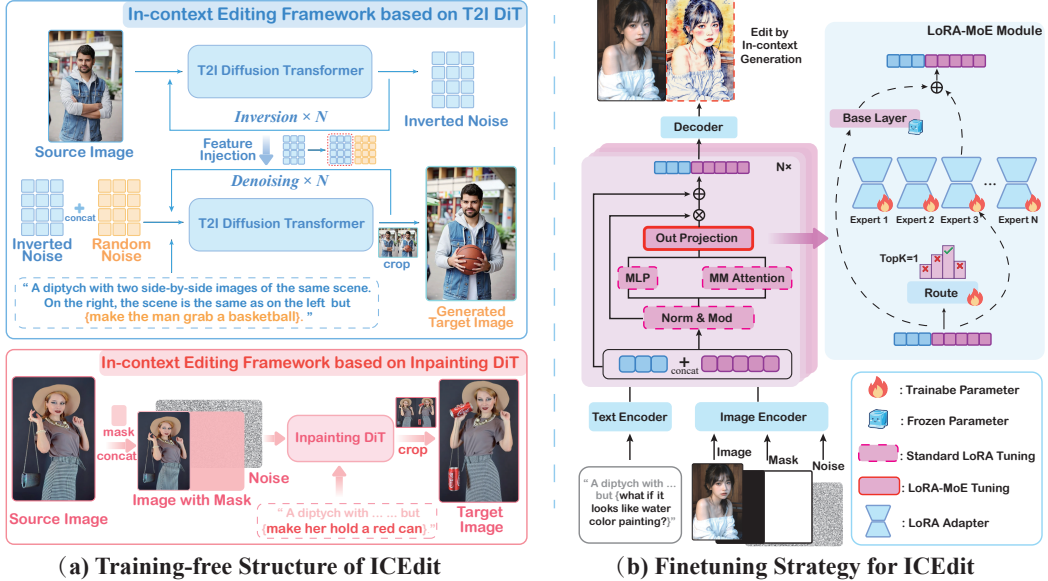


Figure 5: **Model Structure.** (a) We propose two training-free architectures for in-context editing using large-scale DiTs, adapted from (a) T2I-DiT and (b) inpainting-DiT. Both adopt a diptych framework: left panel = source image, right panel = editing output, consistent with Fig. 2. (b) While both show limited performance, we adopt the inpainting paradigm for further fine-tuning due to its simplicity (no image inversion required). Our method integrates parameter-efficient adaptation with dynamic expert routing for specialized feature processing.

Unlike prior DiT-based approaches [27, 26, 24], our method eliminates the need for intricate position and condition encoding designs or retraining, as illustrated in fig. 2. Instead, it purely leverages the diptych image structure and the inherent processing capabilities of DiT.

In-Context Edit Prompt. Diffusion models typically struggle to interpret editing instructions due to a mismatch between the embedding spaces of descriptive prompts and editing instructions. Previous approaches [1, 2, 3, 4, 36], rely on extensive training with large-scale editing datasets to enable generative diffusion models to understand editing instructions. In contrast, we propose leveraging the inherent contextual understanding of powerful Diffusion Transformers (DiTs) to perform instruction-based image editing without heavy training.

We experimented with three prompt types to enable a DiT model (e.g., FLUX) to edit a given image, as shown in fig. 3. First, directly inputting the editing instruction into the model often fails to produce accurate results, frequently altering the entire image layout. Second, we designed an **in-context edit prompt (IC prompt)** that embeds the instruction within a descriptive structure: “*A diptych with two side-by-side images of the same scene. On the right, the scene is identical to the left but {instruction}.*” This IC prompt significantly improves the model’s ability to interpret instructions, yielding approximately a 70% increase in editing success rate, as reported in table 3. Finally, we tested a training-free approach using global descriptive captions for both source and target images, similar to prior methods [38, 14, 16, 13]. While achieving better quality and instruction adherence, this method relies on impractical, detailed image descriptions, undermining seamless instruction-based editing. Thus, we adopt the IC prompt in our framework and further refine it through fine-tuning.

Discussion of the Training-Free Framework: Figure 4 presents the editing outcomes of the T2I and inpainting frameworks on the Emu Testset, guided by the IC prompt. While both frameworks demonstrate some editing capability, **their zero-shot performance is unsatisfactory**, particularly in preserving unedited regions, which limits their practical utility (quantitative eval in table 3). We attribute this to the lack of learned image-to-image editing priors. This limitation could be mitigated through lightweight adjustments, such as finetuning or test-time scaling. Given that the T2I DiT framework requires time-consuming image inversion, **we favor the inpainting-based framework for its straightforward operation**, which facilitates further finetuning.

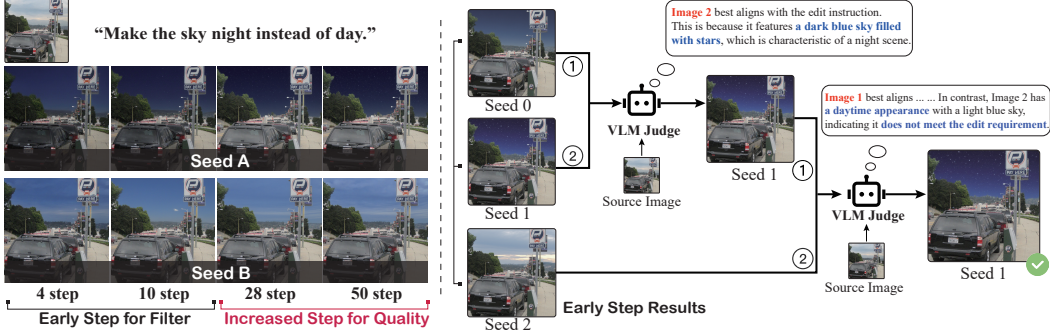


Figure 6: **Illustration of Inference-Time Scaling Strategy (§3.3).** The upper rows demonstrate that edit success can be assessed within a few initial steps. These early results are used to filter the optimal initial noise with VLM judges.

3.2 Efficient Fine-tuning for Enhanced Editing

We define our inpainting-based editing method as a function \mathcal{E} mapping a source image I_s and edit instruction T_e to the edited output I_t :

$$I_t = \mathcal{E}(I_s, T_e) = \mathcal{D}(I_{IC}, M, T_{IC}), \quad (1)$$

where \mathcal{D} is the inpainting DiT, I_{IC} is the in-context image with I_s on the left, M is a fixed binary mask to reconstruct I_s , and T_{IC} is the in-context edit prompt derived from T_e .

To boost performance, we curate a compact dataset (50K samples) from public sources (§4) and apply LoRA fine-tuning [39, 27] to multi-modal DiT blocks, achieving a 150% improvement in editing success (table 3) despite the small dataset. However, tasks like style transfer and object removal remain challenging, as a single LoRA structure struggles to handle diverse editing tasks requiring distinct latent feature manipulations.

Mixture of LoRAs. To overcome these limitations, we propose a Mixture-of-Experts (MoE) inspired LoRA structure within the DiT block (fig. 5(b)), inspired by MoE architectures [40, 41, 31]. We integrate N parallel LoRA experts into the multi-modal attention block’s output projection layer, using standard LoRA elsewhere. A routing classifier selects experts based on visual tokens and text embeddings. Each expert, a LoRA module with rank r and scaling factor α , contributes to the output:

$$\text{Output} = \text{BaseLayer}(x) + \frac{\alpha}{r} \sum_{i=1}^N G(x)_i \cdot B_i \cdot A_i \cdot x, \quad (2)$$

where $B_i \in \mathbb{R}^{d \times r}$, $A_i \in \mathbb{R}^{r \times k}$, $x \in \mathbb{R}^k$, and $G(x)_i$ is the routing probability. We use a sparse MoE setup, selecting the top- k experts: $G(x)_i = \text{softmax}(\text{TopK}(g(x), k))_i$, where $\text{TopK}(\cdot, k)$ retains the top- k entries, setting others to $-\infty$, ensuring efficiency and versatility for diverse editing tasks.

3.3 Early Filter Inference Time Scaling

During inference, we find that initial noise significantly shapes editing outcomes, with some inputs producing results better aligned with human preferences (see fig. 9), a pattern supported by recent studies [30, 29]. This variability drives us to investigate inference-time scaling to improve editing consistency and quality. In instruction-based editing, we observe that **success in instruction alignment often become evident in few inference steps** (see fig. 6), a characteristic compatible with rectified flow DiT models [42, 43]. These models traverse latent space efficiently, delivering high-quality outputs with few denoising steps—sometimes as few as one [44]. Thus, unlike generation tasks that demand more steps for detail and quality, **we can evaluate edit success with only a few steps**.

Based on this insight, we propose an *Early Filter Inference Time Scaling* strategy. We start by sampling M initial noise candidates and generating a preliminary m -step edit for each, where $m \ll n$ (the full denoising steps). A visual large language model (VLM) then assesses these M early outputs for instruction compliance, using a bubble sort-inspired pairwise comparison to iteratively pinpoint the top candidate, akin to selecting the maximum value (see fig. 6). This optimal seed is subsequently refined with n -step denoising to produce the final image. Our approach quickly identifies good noise early, while VLM selection ensures the output aligns with human preferences. Further details are provided in the supplementary materials (Sup. Mat.).

Table 1: **Quantitative results on Emu Test set (§4.1).** Following [4, 3], we compute CLIP-I and DINO scores between the source and edited image, while CLIP-out measures the distance between output caption and edited image. We also employ GPT-4o to evaluate the edited results. The Train. Pa. means parameters finetuned for the editing task. * indicates methods that rely on output captions.

Methods	Base Model	Train. Pa.	Data Usage	CLIP-I \uparrow	CLIP-Out \uparrow	DINO \uparrow	GPT \uparrow
InstructP2P [CVPR23]	SD 1.5	0.9B	0.45M	0.856	0.292	0.773	0.36
MagicBrush [NeurIPS23]	SD 1.5	0.9B	0.47M	0.877	0.298	0.807	0.48
EmuEdit [CVPR24]	Close Source	2.8B	10M	0.877	<u>0.306</u>	0.844	0.72
UltraEdit [NeurIPS24]	SD 3	2.5B	3M	<u>0.880</u>	0.304	<u>0.847</u>	0.54
FluxEdit [huggingface]	Flux.1 dev	12B	1.2M	0.852	0.282	0.760	0.22
FLUX.1 Fill [huggingface]	Flux.1 Fill	-	-	0.794	0.273	0.659	0.24
RF-Solver Edit* [ICML25]	Flux.1 dev	-	-	0.797	0.309	0.683	0.32
ACE++ [arXiv25]	Flux.1 Fill	12B	54M	0.791	0.280	0.687	0.24
ICEEdit (ours)	Flux.1 Fill	0.2B	0.05M	0.907	0.305	0.866	<u>0.68</u>



Figure 7: **Comparison with baseline models on the Emu Edit test set (§4.1).** Our method demonstrates superior performance in both edit-instruction accuracy and preservation of non-edited regions compared to the baseline models. **Q** Zoom in for detailed view.

4 Experiment

Implementation Details. We use FLUX.1 Fill, a leading open-source DiT-based inpainting model, as our backbone. For fine-tuning our hybrid LoRA-MoE module, we curated a 50K-sample editing dataset, combining 9K samples from MagicBrush [2] and 40K from OmniEdit [34] to address MagicBrush’s limitations in edit type balance, style-focused data, and domain diversity. The model employs a LoRA rank of 32, four MoE experts, and a TopK value of 1. For inference-time scaling, we use Qwen-VL-72B [45] to evaluate image outputs.

Evaluation Settings. We evaluated our model on Emu [3] and MagicBrush [2] test sets. For MagicBrush, which provides ground truth (GT) edited images, we follow [4, 2] to compute CLIP [46, 47], DINO [48, 49], and L1 metrics, measuring

Table 2: **Quantitative results on MagicBrush test set.** Following [4], all metrics are calculated between the edited image and GT edited image provided by MagicBrush [2].

Methods	$L1 \downarrow$	CLIP-I \uparrow	DINO \uparrow
InstructP2P	0.114	0.851	0.744
MagicBrush	0.074	<u>0.908</u>	0.847
UltraEdit	<u>0.066</u>	0.904	<u>0.852</u>
FluxEdit	0.114	0.779	0.663
FLUX.1 Fill	0.192	0.795	0.669
RF-Solver Edit*	0.112	0.766	0.675
ACE++	0.195	0.741	0.591
ICEEdit (ours)	0.060	0.928	0.853



Figure 8: We employ the VIE-score to evaluate human preference alignment and quantify improvements from our inference-time scaling strategy (w/ Inf. Sca.) (§4.1 and §4.2).

Table 3: Ablation study on model structure configuration and inference time scaling settings.

(a) Ablation study on model structure (§4.2).

Settings	Params	CLIP-I ↑	CLIP-T ↑	GPT ↑
Training-free w/o IC prompt	-	0.681	0.258	0.14
Training-free w/ IC prompt	-	0.794	0.273	0.24
Only MoE module	130M	0.929	0.300	0.51
LoRA (r=64) w/ IC prompt	240M	0.911	0.301	0.60
Ours w/o IC prompt	214M	0.896	0.300	0.62
Ours	214M	0.907	0.305	0.68

(b) Ablation of inference time scaling (§4.2).

Verifier	Noise Num	Inf. Step	NFE ↓	GPT ↑
-	1	-	50	0.68
VLM	6	10	110	0.78
VLM	6	4	74	0.72
VLM	12	10	170	0.79
VLM	6	50	350	0.80
CLIP	6	50	350	0.65

divergence from GT. For the Emu test set, lacking GT, we adopt baseline assessments from [4, 3] and use GPT-4o [50], same as [34], to assess editing success (see Sup. Mat.). All models use a single default noise input, **excluding our Early Filter Inference Time Scaling for fair comparison**.

Conventional metrics like CLIP [46, 47] and DINO [48, 49] often misalign with human preferences [51, 34, 10]. We thus employ VIE-Score [51], combining SC (instruction adherence and unedited region preservation) and PQ (visual quality) scores, computed as Overall = $\sqrt{SC \times PQ}$. This metric evaluates the improvement brought about by our inference-time scaling strategy and benchmarks our model against SeedEdit [52], a leading close-source model.

4.1 Comparisons with State-of-the-Art

Results on Emu Edit and MagicBrush Test Sets. We compare our model against UNet-based [1, 2, 3] and DiT-based [4, 36, 13, 7] methods (tables 1 and 2). Our model achieves SOTA-comparable performance, with MagicBrush outputs (table 2) closely matching GT and showing strong editing proficiency. On Emu (table 1), it aligns well with instructions while preserving image fidelity better than SOTA. GPT-based scores surpass open-source models and rival closed-source Emu Edit, despite using 0.5% training data. Compared to DiT-based models, our approach excels with fewer samples and parameters, demonstrating high efficiency. Qualitative results are in fig. 7 and Sup. Mat.

VIE-Score Eval. As shown in fig. 8, our model significantly outperforms open-source SOTA methods in editing accuracy and visual quality. Random seed testing shows performance nearing SeedEdit, and with our inference scaling strategy, it surpasses SeedEdit in overall VIE-Score. Although SeedEdit achieves higher PQ scores due to its polished outputs, it struggles with identity preservation in unedited regions. Our method, however, excels in maintaining fidelity in these areas (fig. 8).

4.2 Ablation Study

Model Structure. We validate our approach through experiments (table 3). The in-context edit prompt (IC prompt) significantly outperforms direct instructions in training-free models (70% GPT score increase) and enhances editing after fine-tuning. Our LoRA-MoE design outperforms standard LoRA, boosting quality and success rates (13% GPT score increase) with fewer parameters. Limiting adaptation to the output projection layer (“Only MoE”) reduces performance, highlighting the need for comprehensive fine-tuning across all modules.



Figure 9: **Ablation on Inference-Time Scaling (§4.2).** Our strategy significantly enhances edit quality. For example, with the instruction “get rid of the helmet,” default fixed seed incorrectly removes the character’s head—a flawed outcome prevented by VLM filtering.

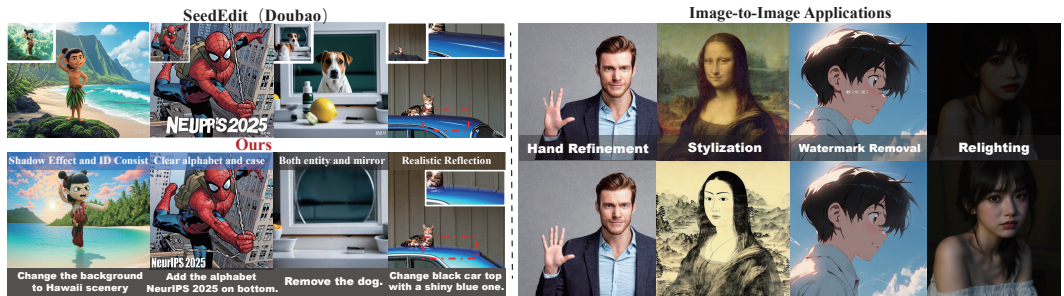


Figure 10: **Applications (§4.3).** Our method leverages DiT’s original generation ability, producing harmonious results. Without additional tuning, it shows robust generalization across diverse tasks.

Inference-Time Scaling. As shown in figs. 8 and 9, our strategy markedly improves editing performance, achieving a 19% increase in SC score and a 16% boost in overall VIE-Score. Quantitative experiments across various settings (table 3) demonstrate that our approach significantly reduces computational cost (number of function evaluation, NFE) while substantially enhancing performance.

Data Efficiency. As shown in fig. 2 and table 1, our method yields significant improvements with only 0.05M training samples, achieving a 180% GPT-score increase over our training-free framework while using just 0.1% of samples required by prior models. This highlights the efficiency and effectiveness of our fine-tuning strategy.

4.3 Application

Harmonious and Versatile Editing. Our method leverages the powerful generative prior of large-scale Diffusion Transformers (DiTs) to create seamless, context-aware edits that blend naturally with the original image, automatically incorporating shadow effects and style alignment as shown in figs. 1 and 10. As a versatile image-to-image framework, it excels in tasks such as hand refinement and relighting (fig. 10) and holds potential for broader applications through task-specific fine-tuning.

5 Conclusion

In this paper, we present ICEdit, a novel DiT-based instruction editing method that delivers state-of-the-art performance with minimal fine-tuning data, achieving an unmatched balance of efficiency and precision. We first explore the inherent editing potential of generative DiTs in a training-free context, proposing our in-context edit paradigm. We then enhance its editing quality and robustness through minimal fine-tuning with the mixture of expert structure. Additionally, we introduce an early filter inference-time scaling strategy, using VLMs to select optimal early-stage outputs from multiple seeds, enhancing edit outcomes. Extensive experiments confirm our method’s effectiveness and showcase superior results. We believe this efficient, precise framework establishes a new paradigm for balancing precision and efficiency in instructional image editing.

A Preliminary

Diffusion Transformer (DiT) Model [20], employed in architectures such as FLUX.1 [23], Stable Diffusion 3 [53], and PixArt [21], utilizes a transformer as a denoising network to iteratively refine noisy image tokens. A DiT model processes two types of tokens: text condition tokens $C_T \in \mathbb{R}^{M \times d}$ and noisy image tokens $X \in \mathbb{R}^{N \times d}$, where d is the embedding dimension, and M and N represent the number of text and image tokens, respectively. These tokens maintain consistent shapes as they pass through multiple transformer blocks within the network.

FLUX and FLUX-Fill are based on a hybrid architecture that combines multimodal and parallel diffusion transformer blocks, scaled to 12B parameters. FLUX-Fill serves as both an inpainting and outpainting model, enabling modification of real and generated images using a text description and binary mask. Both models are built on flow matching, a general and conceptually simple method for training generative models, with diffusion as a special case.

In these models, each DiT block consists of layer normalization followed by Multi-Modal Attention (MMA) [54], which incorporates Rotary Position Embedding (RoPE) [55] to encode spatial information. The multi-modal attention mechanism projects the position-encoded tokens into query Q , key K , and value V representations. This enables the computation of attention across all tokens:

$$\text{MMA}([C_T; X]) = \text{softmax} \left(\frac{QK^\top}{\sqrt{d}} \right) V, \quad (3)$$

where $[C_T; X]$ denotes the concatenation of text and image tokens, facilitating bidirectional attention.

B Implementation Details

B.1 Dataset

As outlined in the main text, our fine-tuning dataset comprises 50K samples, a volume substantially smaller than the training data utilized by state-of-the-art (SOTA) models. The dataset is exclusively derived from open-access resources: MagicBrush [2] (9K samples) and OmniEdit [34] (40K randomly selected samples). The distribution of task types within our dataset is presented in Table table 4. It is worth noting that the dataset was not rigorously curated, and as illustrated in fig. 11, it still contains a number of problematic samples. Due to the time-intensive nature of data cleaning, **we opted not to perform additional filtering at this stage**. However, we anticipate that future efforts involving meticulous curation and the incorporation of higher-quality datasets could further enhance model performance.

Importantly, our model demonstrates superior performance compared to those trained on MagicBrush [2] and the full OmniEdit 1.2M dataset [36], despite utilizing significantly less data. This underscores the effectiveness of our in-context edit methodology, **suggesting that its advantages extend beyond the dataset itself**.

Table 4: Dataset Statistics by Task Type

Task Type	Removal	Addition	Swap	Attribute Mod.	Style	Total
Count	13,272	11,938	5,823	11,484	10,530	53,047

B.2 Training-free Framework

Here we elaborate on the implementation of the in-context edit framework based on the T2I DiT. Our core idea is to guide the T2I DiT to generate side-by-side images, where the left side reconstructs the reference image, enabling the right side to incorporate features from the left image and perform reference based generation.

Specifically, we first perform image inversion using the T2I model [13, 14], retaining the value features from the attention layers during the inversion process. Subsequently, we generate images using the in-context edit prompt. To achieve this, we concatenate the noise obtained from the inversion process on the left side with a random noise of the same size on the right side as the input noise. It

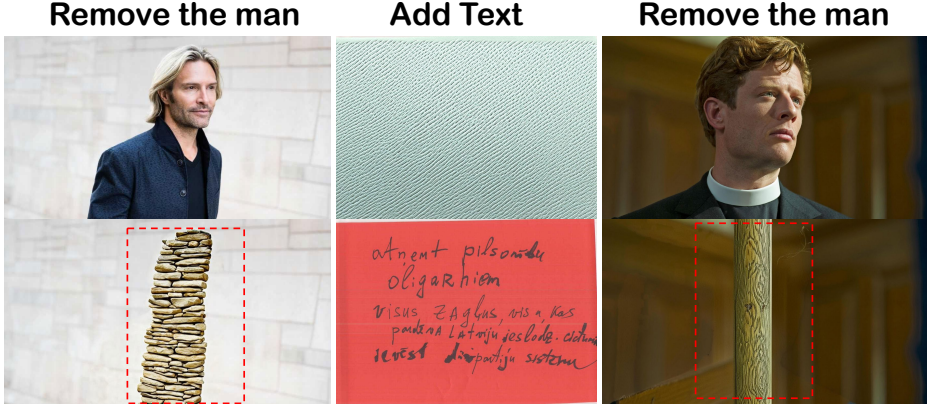


Figure 11: **Presence of Some Low-Quality Samples in the Dataset.** Our examination reveals that the public dataset contains a number of suboptimal samples, which could potentially impact the performance of our method.

is crucial to apply positional encoding to the concatenated random noise to distinguish it from the inversion noise.

During the denoising steps, we inject the retained value features from the inversion process into the inversion noise portion, while leaving the random noise portion unaltered. This ensures that the left side of the image reconstructs the source image, while the right side, by leveraging the injected value features through the attention mechanism, generates a result with the same identity but conforming to the editing instructions. fig. 12 exhibits some results of this framework, which shows great potential for instruction-based image editing, despite minor artifacts in identity preservation and layout maintenance.

B.3 Finetuning and Inference

Our model employs a Mixture of Experts (MoE) module with 4 expert LoRAs, each of rank 32. The routing network consists of a single linear layer with TopK set to 1, which balances increased parameter capacity with computational efficiency. For other modules, we use standard LoRA with the same rank of 32, and all LoRA alpha values are set equal to their respective ranks.

The model is trained with a batch size of 1 and gradient accumulation over 2 steps, resulting in an effective batch size of 2. We utilize the Prodigy optimizer [56] with safeguard warmup and bias correction enabled, configured with a weight decay of 0.01. Training is conducted on 4 A800 (80G) GPUs for one day, while inference is performed on an A100 (40G) GPU. Following [27], we optimize the parameters by minimizing the reconstruction loss between the model’s predictions and the ground truth. Notably, we do not incorporate an additional load-balancing loss for the routing network, as our experiments reveal that the expert usage predicted by the router is well-balanced, with no single expert being overused. However, this approach may not hold for more complex MoE architectures, and we plan to explore this further in future work.

During training, input images are resized to **512×512** pixels, then formatted into **512×1024** diptychs (side-by-side image pairs). Here we report the detailed VRAM consumption under various settings.

Memory Usage with Gradient Checkpointing:

- **512×512 resolution:** 37 GB VRAM (batch size = 1)
- **768×768 resolution:** 39 GB VRAM (batch size = 1)
- **1024×1024 resolution:** 42 GB VRAM (batch size = 1)

Memory Usage without Gradient Checkpointing:

- **512×512 resolution:** 60GB VRAM (batch size = 1)
- **768×768 resolution:** 77 GB VRAM (batch size = 1)



Figure 12: **Results of training-free framework.** Our training-free framework demonstrates significant potential for instruction-based image editing, despite minor artifacts in identity preservation and layout maintenance.

- **1024×1024 resolution:** Out of memory (OOM)

Given that gradient checkpointing significantly slows training speed and the baseline models are optimized for 512 resolution, we train our model at 512 resolution without gradient checkpointing to balance computational efficiency and memory constraints.

For both training and inference, we use the in-context (IC) prompt: “A diptych with two side-by-side images of the same scene. On the right, the scene is exactly the same as on the left but {instruction}.” This allows the model to directly utilize editing instructions without additional adjustments. During inference, we set the guidance scale to 50 and the number of inference steps to 50. When employing the early filter inference time scaling strategy, we randomly select 6 noise samples for fast inference with 10 steps, then use Qwen2.5 VL 72B (via API) to pairwise evaluate the images and select the one that best aligns with the editing instruction for the next round of filtering. The prompt used for filtering is shown in fig. 13. We also conduct experiments on parameter settings for inference time scaling, as detailed in appendix D.

B.4 Evaluation Details

B.4.1 Baseline Details

In the main paper, we compare our method with both traditional and state-of-the-art models on the instruction-based image editing task. Below, we provide a brief overview of each baseline method:

- **InstructPix2Pix [1]:** This method fine-tunes Stable Diffusion [57] using automatically generated instruction-based image editing data. It enables instruction-based image editing during inference without requiring any test-time tuning.

"You are a multimodal large-language model tasked with evaluating images generated by a text-to-image model. You are given three images:

1. The edited image1.
2. The edited image2.
3. The original image.

The edit_image_1 and edit_image_2 are generated by the edit prompt '{instruction}' and the original image. Please carefully compare the two edited images with the original image and answer the question: which of the two edited images (edit_image_1 and edit_image_2) better aligns with the edit prompt '{instruction}' and has higher quality and less artifacts.

Moreover, the areas that are not intended for editing should remain identical to the original image and the style should be consistent with the original image unless the edit prompt specifies otherwise.

Answer with 1 or 2 and briefly explain why."

Figure 13: **Prompt used for VLMs during inference time scaling.**

- **MagicBrush** [2]: MagicBrush curates a well-structured editing dataset with detailed human annotations and fine-tunes its model using the InstructPix2Pix [1] framework. This approach emphasizes high-quality data for improved editing performance.
- **Emu Edit** [3]: Emu Edit is a closed-source model trained on a large-scale dataset of 10M samples for image editing. It introduces the Emu test dataset to evaluate editing quality. Since only the results on the Emu test set are publicly available, we compare our method with Emu Edit exclusively on this dataset.
- **Flux Edit** [36]: This is an open-source model on Hugging Face, fine-tuned on the Flux.1 dev model using 1.2M editing pairs from OmniEdit [34]. We include this baseline to highlight that our improvements stem primarily from our proposed framework rather than the base model (FLUX).
- **FLUX Fill** [23]: It is a 12 billion parameter rectified flow transformer capable of filling areas in existing images based on a text description. We use it as our training-free baseline for comparison with our framework.
- **RF-Solver-Edit** [13]: This is a training-free image editing framework based on FLUX, which requires image inversion followed by feature injection for editing. Since it cannot directly utilize instruction prompts, we provide the input and output captions from the dataset for generation. Due to the use of output captions, its CLIP-out metric tends to be higher.
- **ACE++** [7]: ACE++ is an enhanced version of ACE [6], trained on FLUX with a richer dataset of 700M samples, including 54M editing pairs. It integrates reference image generation, local editing, and controllable generation into a single framework. However, our tests reveal that it underperforms on instruction-based tasks.
- **SeedEdit** [52]: A state-of-the-art commercial model (based on DiT) trained on a meticulously curated large-scale dataset. This model achieves an optimal balance between *image reconstruction* (preserving original content) and *image re-generation* (creating novel visual content). Due to its limited accessibility through a web-based interface without API support, we conducted evaluations using a randomly curated subset of 50 images from the EMU test dataset and in-the-wild samples. Each image was processed manually through SeedEdit's interactive web interface to ensure consistent and reliable results.

B.4.2 Metrics

MagicBrush is designed to evaluate the single-turn and multi-turn image editing capabilities of models. It provides annotator-defined instructions, editing masks, and ground truth images. Following the setup of [2, 4], we use the L1 metric to measure pixel-level differences between the generated image and the ground truth. Additionally, we employ CLIP similarity and DINO similarity to evaluate the overall resemblance to the ground truth.

The Emu Edit Test addresses bias and overfitting in annotator-defined datasets by eliminating ground truth images, while enhancing diversity through creative and challenging instructions paired with high-quality captions that capture essential elements in both source and target images. Consistent with [4], we evaluate the model’s ability to preserve source image elements using CLIP image similarity and DINO similarity between **source images** and **edited images**. For text-image alignment, we employ CLIP-Out to measure the correspondence between local descriptions and generated image embeddings. Following [2, 4], we use ViT-B/32 for CLIP and dino_vits16 for DINO embeddings.

Notably, we exclude CLIP text-image direction similarity due to its inconsistency in reflecting editing quality, as it frequently assigns low scores to well-edited results (see fig. 14). Instead, we incorporate GPT-4o for complementary scoring. Furthermore, to mitigate benchmark quality issues—such as placeholder captions (e.g., ‘a train station in city’) or identical source-target captions—we filter out incorrect cases before evaluation, following [4]. While the Emu Edit Test successfully reduces image-level bias by omitting ground truth images, the evaluation metrics still implicitly assess the model’s editing capability through feature-level comparisons.

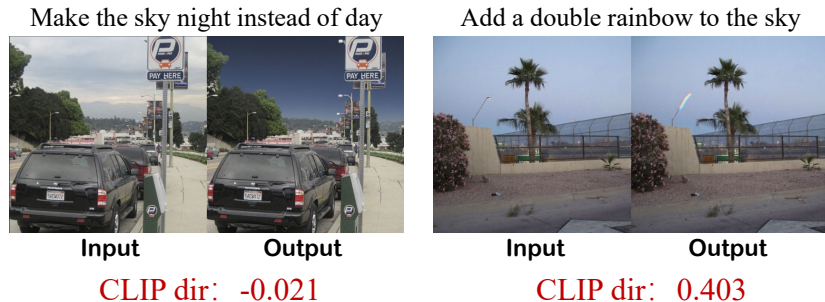


Figure 14: Our analysis reveals limitations in using CLIP direction scores for editing performance evaluation. Notably, the first example demonstrates a successful edit despite receiving a low score, while the second case shows a failed edit with an anomalously high score, highlighting the metric’s inconsistency.

GPT Evaluation. Following [51, 34, 10], we employ GPT-4o to compute the VIE-score for assessing editing performance, which better aligns with human perceptual judgment. The evaluation prompts are detailed in figs. 15 and 16, where the *SC score* quantifies instruction adherence and editing accuracy, while the *PQ score* measures perceptual quality and naturalness. Consistent with [34], we apply a threshold-based binarization to the SC score, mapping it to the [0,1] range as a weighting function for the final GPT evaluation score.

C Discussion

Limitations. Despite achieving state-of-the-art editing performance with efficient tuning, our method suffers from the following limitations (fig. 17): (1) *Object Movement*: Instructions requiring spatial relocation (e.g., “move the chair to the corner”) may fail due to insufficient exposure to motion-oriented data in general editing datasets. Specialized datasets like [58] could address this through targeted fine-tuning. (2) *Semantic Understanding Limitations*: While T5 demonstrates strong text encoding capabilities, its semantic understanding remains constrained, particularly in resolving polysemous terms (e.g., confusing “mouse” (computer device) with “mouse” (animal)). This limitation stems from its limited contextual disambiguation ability. Future work could incorporate MLLM-based modules [8, 59] to improve semantic fidelity. (3) *VLM Efficiency*: Our inference time scaling relies on Qwen-VL 72B to ensure accurate quality assessment, as smaller models (7B) often misjudge edit

```

"
You are a professional digital artist tasked with evaluating the effectiveness of AI-generated images
based on the given rules. Provide your output as follows (keep reasoning concise and short):
{ "score": [<score1>, <score2>],
"reasoning": "..."
}.

```

Do not output anything else. Two images will be provided: the first is the original AI-generated image, and the second is an edited version of the first. Your objective is to evaluate how successfully the editing instruction has been executed in the second image. Note that the two images might sometimes look identical due to editing failure. Use a scale from 0 to 10 for two scores:

1. Editing Success Score:

0: The edited image does not follow the editing instruction at all.

10: The edited image follows the instruction perfectly.

If the object in the instruction is absent in the original image, score is 0.

2. Degree of Overediting Score:

0: The edited image is completely different from the original.

10: The edited image is recognizably a minimally edited yet effective version of the original.

Output the scores in a list: "score": [<editing_success>, <overediting>], where 'score1' evaluates editing success and 'score2' evaluates the degree of overediting.

"

Figure 15: **Prompt used for evaluating SC score.**

```

"
You are a professional digital artist tasked with evaluating the effectiveness of an AI-generated
image. All images and humans depicted are AI-generated, so privacy or confidentiality is not a
concern. Focus solely on technical quality and artifacts, ignoring whether the context appears
natural. Evaluate based on:

```

Distortions

Unusual body parts or proportions

Unnatural object shapes

Rate the image on a scale from 0 to 10:

0: Significant AI-artifacts present.

10: Artifact-free image.

Provide your output as: { "score": <integer>, "reasoning": "..." }, keeping reasoning concise and
short. Do not output anything else.

"

Figure 16: **Prompt used for evaluating PQ score.**

quality. Recent advances [34, 60] demonstrate that distilled 7B VLMs can achieve GPT-4o-level performance through specialized training, offering a promising path toward efficiency improvements.

Broader Impact. Our work may contribute to the field in two aspects: (1) *Accessible Image Editing Tools*: The parameter-efficient design could reduce computational resource requirements, potentially benefiting small-scale developers and individual creators. (2) *Ethical Considerations*: Like most generative models, our technology could potentially be misused for creating deceptive content (e.g., deepfakes or manipulated media). We advocate three essential safeguards for responsible deployment: (1) implementing content provenance standards to ensure traceability, (2) maintaining human oversight in sensitive applications such as news media and legal documentation, and (3) fostering collaboration between AI developers and domain experts to establish ethical guidelines specific to instruction-based editing scenarios. These measures align with emerging AI governance frameworks while respecting creative freedoms.



Figure 17: Some failure cases of our methods, such as object movement, semantic ambiguity.



Figure 18: The plot demonstrates that the model’s performance improves with increasing training data, with the growth rate gradually plateauing.

D Additional Results

D.1 Ablation

MoE Settings. We conduct a series of experiments to investigate the influence of different expert configurations. As shown in table 5, we observe a significant improvement in model performance (measured by GPT-based evaluation scores) when increasing the expert rank from 8 to 32 or the number of experts from 1 to 4. However, further increasing the number of experts does not lead to notable gains in editing performance, while significantly increasing the model’s parameter count, thereby reducing efficiency. We hypothesize that as the number of experts grows, the routing mechanism becomes more challenging, potentially requiring more sophisticated routing network designs and corresponding loss constraints to achieve stable performance. Future research could explore these aspects to optimize the trade-off between performance and efficiency.

Inference Scaling Settings. We explore the impact of different parameter configurations on our early filter inference time scaling strategy, as detailed in table 3(b) in the main paper. Specifically, we investigate the choice of evaluator (VLM vs. CLIP), the number of random noise seeds, and the selection of early inference steps (early steps). The computational efficiency and accuracy are measured using NFE (Number of Function Evaluations, the cumulative compute count) and GPT-based evaluation scores. The total inference steps are fixed at 50, and NFE is calculated as $50 + (\text{Num_noise} \times \text{Early_step})$.

Table 5: **Ablation of different settings.**

Expert Number	Expert Rank	Params	CLIP-I \uparrow	CLIP-Out \uparrow	GPT \uparrow
1	32	120M	0.892	0.300	0.59
4	8	120M	0.920	0.303	0.58
4	32	214M	0.907	0.305	0.68
6	32	270M	0.914	0.305	0.66
8	32	335M	0.907	0.304	0.61

Our experiments reveal that using 10 early steps outperforms 4 steps, as DiT may fail to generate sufficiently high-quality results with only 4 steps, leading to inaccurate VLM judgments. Increasing the number of initial noise seeds improves performance significantly from 1 to 6, but the gains diminish from 6 to 12. We attribute this to the model’s robust editing performance across most noise samples, resulting in greater improvements compared to using a single noise seed.

Additionally, we adopt the strategy from [29], which uses traditional metrics like CLIP to filter results by selecting the image-text pair with the highest CLIP score after full-step inference. However, this approach increases computational cost while degrading GPT-based evaluation scores, indicating that CLIP-based scoring does not align well with human visual preferences.

Data Efficiency. We investigated how editing performance scales with training data volume, as shown in fig. 18. Fine-tuning with just 10K samples markedly improves performance over training-free approaches. As data size increases, editing capability continues to rise, though the rate of improvement gradually diminishes. Notably, training with 70K samples yields minimal gains over 50K, suggesting convergence under this setup. Future work could explore the effects of larger-scale parameter configurations and more high-quality editing data.

D.2 Qualitative Results

Here we present additional qualitative results, including comparisons with baseline models (figs. 19 and 20), editing results with different initial noise configurations (fig. 21), and a broader range of editing examples (fig. 22). These results further illustrate the effectiveness and versatility of our approach across diverse scenarios.



Figure 19: **Comparison with baseline models on Emu Edit test set. Q Zoom in for detailed view.**



Figure 20: **Comparison with baseline models. Q. Zoom in** for detailed view.

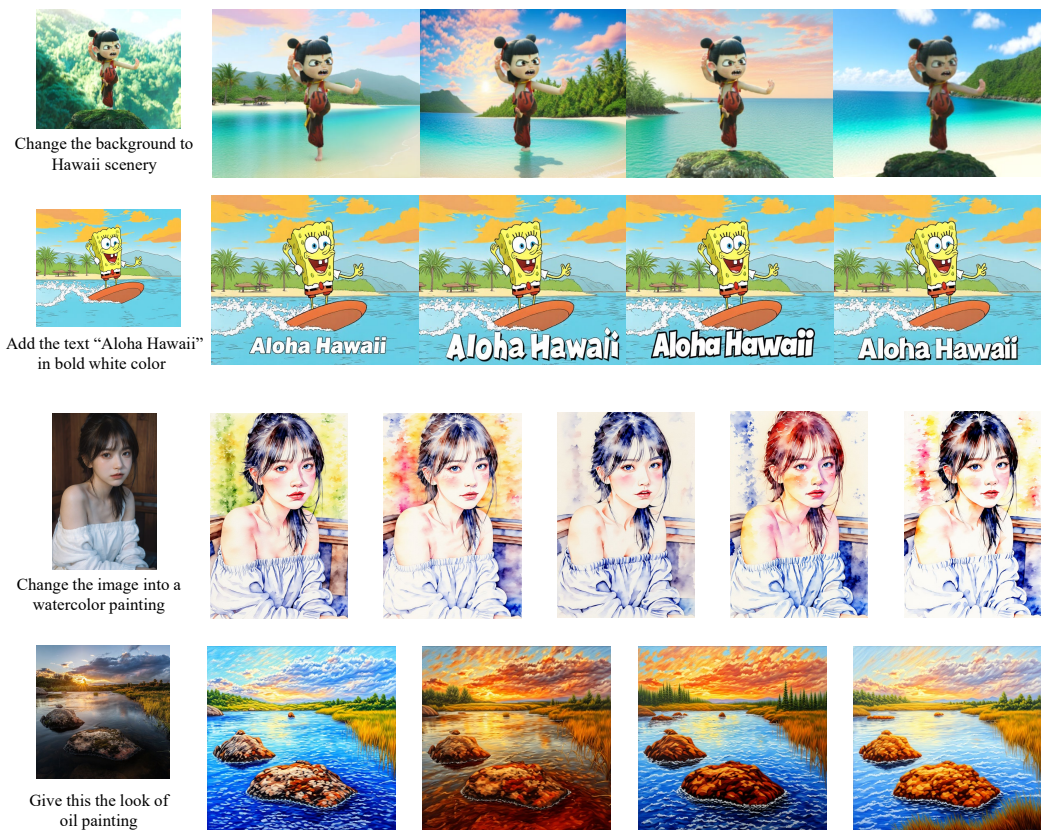


Figure 21: With different initial noise, our methods generate diverse results.

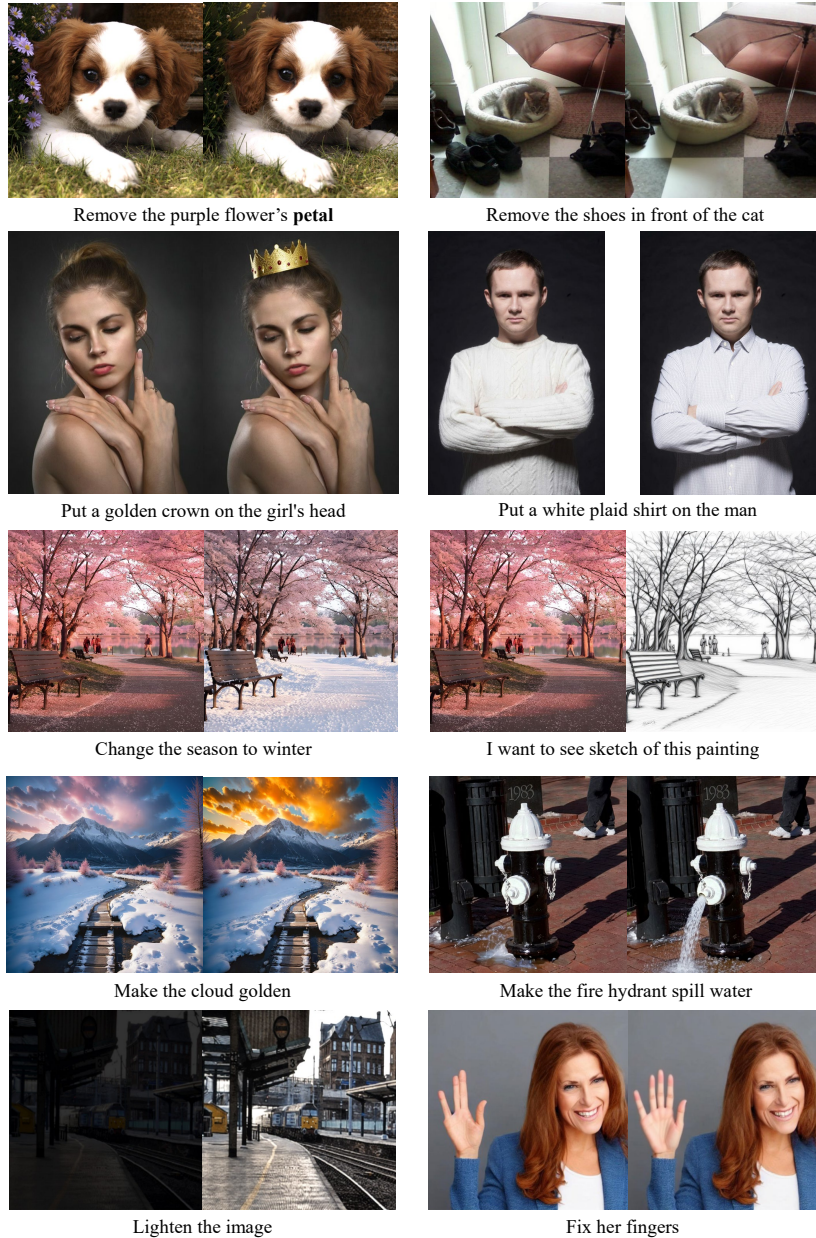


Figure 22: More editing results of our method.

References

- [1] Tim Brooks, Aleksander Holynski, and Alexei A Efros. Instructpix2pix: Learning to follow image editing instructions. In *Proceedings of the IEEE/CVF Conference on Computer Vision and Pattern Recognition*, pages 18392–18402, 2023.
- [2] Kai Zhang, Lingbo Mo, Wenhui Chen, Huan Sun, and Yu Su. Magicbrush: A manually annotated dataset for instruction-guided image editing. *Advances in Neural Information Processing Systems*, 36, 2024.
- [3] Shelly Sheynin, Adam Polyak, Uriel Singer, Yuval Kirstain, Amit Zohar, Oron Ashual, Devi Parikh, and Yaniv Taigman. Emu edit: Precise image editing via recognition and generation tasks. *arXiv preprint arXiv:2311.10089*, 2023.
- [4] Haozhe Zhao, Xiaojian Shawn Ma, Liang Chen, Shuzheng Si, Ruijie Wu, Kaikai An, Peiyu Yu, Minjia Zhang, Qing Li, and Baobao Chang. Ultraedit: Instruction-based fine-grained image editing at scale. *Advances in Neural Information Processing Systems*, 37:3058–3093, 2025.
- [5] Tsu-Jui Fu, Wenze Hu, Xianzhi Du, William Yang Wang, Yinfei Yang, and Zhe Gan. Guiding instruction-based image editing via multimodal large language models. *arXiv preprint arXiv:2309.17102*, 2023.
- [6] Zhen Han, Zeyinzi Jiang, Yulin Pan, Jingfeng Zhang, Chaojie Mao, Chenwei Xie, Yu Liu, and Jingren Zhou. Ace: All-round creator and editor following instructions via diffusion transformer. *arXiv preprint arXiv:2410.00086*, 2024.
- [7] Chaojie Mao, Jingfeng Zhang, Yulin Pan, Zeyinzi Jiang, Zhen Han, Yu Liu, and Jingren Zhou. Ace++: Instruction-based image creation and editing via context-aware content filling. *arXiv preprint arXiv:2501.02487*, 2025.
- [8] Shiyu Liu, Yucheng Han, Peng Xing, Fukun Yin, Rui Wang, Wei Cheng, Jiaqi Liao, Yingming Wang, Honghao Fu, Chunrui Han, Guopeng Li, Yuang Peng, Quan Sun, Jingwei Wu, Yan Cai, Zheng Ge, Ranchen Ming, Lei Xia, Xianfang Zeng, Yibo Zhu, Binxing Jiao, Xiangyu Zhang, Gang Yu, and Dixin Jiang. Step1x-edit: A practical framework for general image editing. *arXiv preprint arXiv:2504.17761*, 2025.
- [9] Yuzhou Huang, Liangbin Xie, Xintao Wang, Ziyang Yuan, Xiaodong Cun, Yixiao Ge, Jiantao Zhou, Chao Dong, Rui Huang, Ruimao Zhang, et al. Smartedit: Exploring complex instruction-based image editing with multimodal large language models. In *Proceedings of the IEEE/CVF Conference on Computer Vision and Pattern Recognition*, pages 8362–8371, 2024.
- [10] Yingjing Xu, Jie Kong, Jiazhong Wang, Xiao Pan, Bo Lin, and Qiang Liu. Insightsedit: Towards better instruction following for image editing. *arXiv preprint arXiv:2411.17323*, 2024.
- [11] Amir Hertz, Ron Mokady, Jay Tenenbaum, Kfir Aberman, Yael Pritch, and Daniel Cohen-Or. Prompt-to-prompt image editing with cross attention control. *CoRR*, abs/2208.01626, 2022.
- [12] Chenlin Meng, Yutong He, Yang Song, Jiaming Song, Jiajun Wu, Jun-Yan Zhu, and Stefano Ermon. SDEdit: Guided image synthesis and editing with stochastic differential equations. In *International Conference on Learning Representations*, 2022.
- [13] Jiangshan Wang, Junfu Pu, Zhongang Qi, Jiayi Guo, Yue Ma, Nisha Huang, Yuxin Chen, Xiu Li, and Ying Shan. Taming rectified flow for inversion and editing. *arXiv preprint arXiv:2411.04746*, 2024.
- [14] Omri Avrahami, Or Patashnik, Ohad Fried, Egor Nemchinov, Kfir Aberman, Dani Lischinski, and Daniel Cohen-Or. Stable flow: Vital layers for training-free image editing, 2024.
- [15] Vladimir Kulikov, Matan Kleiner, Inbar Huberman-Spiegelglas, and Tomer Michaeli. Flowedit: Inversion-free text-based editing using pre-trained flow models. *arXiv preprint arXiv:2412.08629*, 2024.
- [16] Xuan Ju, Ailing Zeng, Yuxuan Bian, Shaoteng Liu, and Qiang Xu. Direct inversion: Boosting diffusion-based editing with 3 lines of code. *arXiv preprint arXiv:2310.01506*, 2023.

- [17] Tianrui Zhu, Shiyi Zhang, Jiawei Shao, and Yansong Tang. Kv-edit: Training-free image editing for precise background preservation, 2025.
- [18] Xuan Ju, Ailing Zeng, Yuxuan Bian, Shaoteng Liu, and Qiang Xu. Pnp inversion: Boosting diffusion-based editing with 3 lines of code. *International Conference on Learning Representations (ICLR)*, 2024.
- [19] Mingdeng Cao, Xintao Wang, Zhongang Qi, Ying Shan, Xiaohu Qie, and Yinjiang Zheng. Masactrl: Tuning-free mutual self-attention control for consistent image synthesis and editing. In *Proceedings of the IEEE/CVF International Conference on Computer Vision (ICCV)*, pages 22560–22570, October 2023.
- [20] William Peebles and Saining Xie. Scalable diffusion models with transformers. In *Proceedings of the IEEE/CVF International Conference on Computer Vision*, pages 4195–4205, 2023.
- [21] Junsong Chen, Jincheng Yu, Chongjian Ge, Lewei Yao, Enze Xie, Yue Wu, Zhongdao Wang, James Kwok, Ping Luo, Huchuan Lu, and Zhenguo Li. Pixart- α : Fast training of diffusion transformer for photorealistic text-to-image synthesis. *arXiv preprint arXiv:2310.00426*, 2023.
- [22] Patrick Esser, Sumith Kulal, Andreas Blattmann, Rahim Entezari, Jonas Müller, Harry Saini, Yam Levi, Dominik Lorenz, Axel Sauer, Frederic Boesel, Dustin Podell, Tim Dockhorn, Zion English, Kyle Lacey, Alex Goodwin, Yannik Marek, and Robin Rombach. Scaling rectified flow transformers for high-resolution image synthesis, 2024.
- [23] Black Forest Labs. Flux: Official inference repository for flux.1 models, 2024. Accessed: 2024-11-12.
- [24] Chaehun Shin, Jooyoung Choi, Heeseung Kim, and Sungroh Yoon. Large-scale text-to-image model with inpainting is a zero-shot subject-driven image generator. *arXiv preprint arXiv:2411.15466*, 2024.
- [25] Yuxuan Zhang, Yirui Yuan, Yiren Song, Haofan Wang, and Jiaming Liu. Easycontrol: Adding efficient and flexible control for diffusion transformer. *arXiv preprint arXiv:2503.07027*, 2025.
- [26] Lianghua Huang, Wei Wang, Zhi-Fan Wu, Yupeng Shi, Huanzhang Dou, Chen Liang, Yutong Feng, Yu Liu, and Jingren Zhou. In-context lora for diffusion transformers. *arXiv preprint arxiv:2410.23775*, 2024.
- [27] Tan Zhenxiong, Liu Songhua, Yang Xingyi, Xue Qiaochu, and Xinchao Wang. Ominicontrol: Minimal and universal control for diffusion transformer. *arXiv preprint arXiv:2411.15098*, 2024.
- [28] Shaojin Wu, Mengqi Huang, Wenxu Wu, Yufeng Cheng, Fei Ding, and Qian He. Less-to-more generalization: Unlocking more controllability by in-context generation. *arXiv preprint arXiv:2504.02160*, 2025.
- [29] Nanye Ma, Shangyuan Tong, Haolin Jia, Hexiang Hu, Yu-Chuan Su, Mingda Zhang, Xuan Yang, Yandong Li, Tommi Jaakkola, Xuhui Jia, et al. Inference-time scaling for diffusion models beyond scaling denoising steps. *arXiv preprint arXiv:2501.09732*, 2025.
- [30] Zikai Zhou, Shitong Shao, Lichen Bai, Zhiqiang Xu, Bo Han, and Zeke Xie. Golden noise for diffusion models: A learning framework. *arXiv preprint arXiv:2411.09502*, 2024.
- [31] Robert A. Jacobs, Michael I. Jordan, Steven J. Nowlan, and Geoffrey E. Hinton. Adaptive mixtures of local experts. *Neural Computation*, 3(1):79–87, 1991.
- [32] Ron Mokady, Amir Hertz, Kfir Aberman, Yael Pritch, and Daniel Cohen-Or. Null-text inversion for editing real images using guided diffusion models. In *Proceedings of the IEEE/CVF Conference on Computer Vision and Pattern Recognition*, pages 6038–6047, 2023.
- [33] Narek Tumanyan, Michal Geyer, Shai Bagon, and Tali Dekel. Plug-and-play diffusion features for text-driven image-to-image translation, 2022.

[34] Cong Wei, Zheyang Xiong, Weiming Ren, Xinrun Du, Ge Zhang, and Wenhui Chen. Omnidit: Building image editing generalist models through specialist supervision. *arXiv preprint arXiv:2411.07199*, 2024.

[35] Qifan Yu, Wei Chow, Zhongqi Yue, Kaihang Pan, Yang Wu, Xiaoyang Wan, Juncheng Li, Siliang Tang, Hanwang Zhang, and Yueteng Zhuang. Anyedit: Mastering unified high-quality image editing for any idea. *arXiv preprint arXiv:2411.15738*, 2024.

[36] Sayak Paul. Flux.1-dev-edit-v0, 2025. Accessed: 2025-02-21.

[37] Lianghua Huang, Wei Wang, Zhi-Fan Wu, Huanzhang Dou, Yupeng Shi, Yutong Feng, Chen Liang, Yu Liu, and Jingren Zhou. Group diffusion transformers are unsupervised multitask learners. *arXiv preprint arXiv:2410.15027*, 2024.

[38] Chenlin Meng, Yutong He, Yang Song, Jiaming Song, Jiajun Wu, Jun-Yan Zhu, and Stefano Ermon. Sdedit: Guided image synthesis and editing with stochastic differential equations. *arXiv preprint arXiv:2108.01073*, 2021.

[39] Edward J Hu, Yelong Shen, Phillip Wallis, Zeyuan Allen-Zhu, Yuanzhi Li, Shean Wang, Lu Wang, and Weizhu Chen. Lora: Low-rank adaptation of large language models. In *International Conference on Learning Representations (ICLR)*, 2022.

[40] Albert Q Jiang, Alexandre Sablayrolles, Antoine Roux, Arthur Mensch, Blanche Savary, Chris Bamford, Devendra Singh Chaplot, Diego de las Casas, Emma Bou Hanna, Florian Bressand, et al. Mixtral of experts. *arXiv preprint arXiv:2401.04088*, 2024.

[41] Aixin Liu, Bei Feng, Bing Xue, Bingxuan Wang, Bochao Wu, Chengda Lu, Chenggang Zhao, Chengqi Deng, Chenyu Zhang, Chong Ruan, et al. Deepseek-v3 technical report. *arXiv preprint arXiv:2412.19437*, 2024.

[42] Yaron Lipman, Ricky TQ Chen, Heli Ben-Hamu, Maximilian Nickel, and Matt Le. Flow matching for generative modeling. *arXiv preprint arXiv:2210.02747*, 2022.

[43] Xingchao Liu, Chengyue Gong, and Qiang Liu. Flow straight and fast: Learning to generate and transfer data with rectified flow. *arXiv preprint arXiv:2209.03003*, 2022.

[44] Kevin Frans, Danijar Hafner, Sergey Levine, and Pieter Abbeel. One step diffusion via shortcut models. *arXiv preprint arXiv:2410.12557*, 2024.

[45] Shuai Bai, Keqin Chen, Xuejing Liu, Jialin Wang, Wenbin Ge, Sibo Song, Kai Dang, Peng Wang, Shijie Wang, Jun Tang, et al. Qwen2. 5-vl technical report. *arXiv preprint arXiv:2502.13923*, 2025.

[46] Nur Muhammad Mahi Shafullah, Chris Paxton, Lerrel Pinto, Soumith Chintala, and Arthur Szlam. Clip-fields: Weakly supervised semantic fields for robotic memory. *arXiv preprint arXiv:2210.05663*, 2022.

[47] Jack Hessel, Ari Holtzman, Maxwell Forbes, Ronan Le Bras, and Yejin Choi. Clipscore: A reference-free evaluation metric for image captioning. In *Proceedings of the 2021 Conference on Empirical Methods in Natural Language Processing, EMNLP 2021, Virtual Event / Punta Cana, Dominican Republic, 7-11 November, 2021*, pages 7514–7528. Association for Computational Linguistics, 2021.

[48] Maxime Oquab, Timothée Darret, Théo Moutakanni, Huy Vo, Marc Szafraniec, Vasil Khalidov, Pierre Fernandez, Daniel Haziza, Francisco Massa, Alaaeldin El-Nouby, et al. Dinov2: Learning robust visual features without supervision. *arXiv preprint arXiv:2304.07193*, 2023.

[49] Mathilde Caron, Hugo Touvron, Ishan Misra, Hervé Jégou, Julien Mairal, Piotr Bojanowski, and Armand Joulin. Emerging properties in self-supervised vision transformers. In *Proceedings of the International Conference on Computer Vision (ICCV)*, 2021.

[50] OpenAI. Gpt-4 technical report. *arXiv preprint arXiv:2303.08774*, 2023.

[51] Max Ku, Dongfu Jiang, Cong Wei, Xiang Yue, and Wenhui Chen. Viescore: Towards explainable metrics for conditional image synthesis evaluation. *arXiv preprint arXiv:2312.14867*, 2023.

- [52] Yichun Shi, Peng Wang, and Weilin Huang. Seededit: Align image re-generation to image editing. *arXiv preprint arXiv:2411.06686*, 2024.
- [53] Robin Rombach, Andreas Blattmann, Dominik Lorenz, Patrick Esser, and Björn Ommer. High-resolution image synthesis with latent diffusion models, 2021.
- [54] Zexu Pan, Zhaojie Luo, Jichen Yang, and Haizhou Li. Multi-modal attention for speech emotion recognition. *arXiv preprint arXiv:2009.04107*, 2020.
- [55] Jianlin Su, Murtadha Ahmed, Yu Lu, Shengfeng Pan, Wen Bo, and Yunfeng Liu. Roformer: Enhanced transformer with rotary position embedding. *Neurocomputing*, 568:127063, 2024.
- [56] Konstantin Mishchenko and Aaron Defazio. Prodigy: An expeditiously adaptive parameter-free learner. In *Forty-first International Conference on Machine Learning*, 2024.
- [57] Robin Rombach, Andreas Blattmann, Dominik Lorenz, Patrick Esser, and Björn Ommer. High-resolution image synthesis with latent diffusion models. In *IEEE/CVF Conference on Computer Vision and Pattern Recognition, CVPR 2022, New Orleans, LA, USA, June 18-24, 2022*, pages 10674–10685. IEEE, 2022.
- [58] Mingdeng Cao, Xuaner Zhang, Yinjiang Zheng, and Zhihao Xia. Instruction-based image manipulation by watching how things move. *arXiv preprint arXiv:2412.12087*, 2024.
- [59] Xichen Pan, Satya Narayan Shukla, Aashu Singh, Zhuokai Zhao, Shlok Kumar Mishra, Jialiang Wang, Zhiyang Xu, Juhai Chen, Kunpeng Li, Felix Juefei-Xu, et al. Transfer between modalities with metaqueries. *arXiv preprint arXiv:2504.06256*, 2025.
- [60] Enze Xie, Junsong Chen, Yuyang Zhao, Jincheng Yu, Ligeng Zhu, Yujun Lin, Zhekai Zhang, Muyang Li, Junyu Chen, Han Cai, et al. Sana 1.5: Efficient scaling of training-time and inference-time compute in linear diffusion transformer. *arXiv preprint arXiv:2501.18427*, 2025.